www.RedMountainRadio.com

Thanks for your interest in my technical paper. If you find this work to be interesting, or have additional questions, please contact me at the address below. Red Mountain Radio LLC offers professional RF, optical, and microwave design services, and problem solving.

Regards,
Eric Funk, Ph. D.
Partner, Red Mountain Radio LLC
eric@redmountainradio.com
970-325-2158 ×12

Session TSC6

MICROWAVE PHOTONICS

Performance Limits of a Hybrid Fiber/Millimeter-Wave Wireless System

Eric E. Funk, P. R. Herczfeld, W. D. Jemison and Maja Bystrom

Performance Limits of a Hybrid Fiber/Millimeter-Wave Wireless System

Eric E. Funk, P. R. Herczfeld, W. D. Jemison and Maja Bystrom

Abstract — **This paper reports a physical layer performance analysis for a hybrid fiber/wireless millimeter-wave communications system. The impact of the fiber link is carefully considered together with the microwave link budget. Vector modulation measurements are used to assess the quality of the fiber link.**

Index Terms — **millimeter-wave, fiber radio, LMDS, vector modulation.**

I. Introduction

Today, the demand for high-speed wireless connectivity, together with the large available bandwidth at millimeter-wave frequencies has led to the development of fixed cellular point-to-multipoint millimeter wave services such as the 28 GHz Local Multipoint Distribution Service (LMDS) in the U.S. This type of wireless connectivity is also of interest to the US Navy for shipboard communications due to the increased security (directionality/ attenuation) of millimeter wave signals.

While LMDS subscriber equipment is designed for low-cost, LMDS basestations are still extremely costly to deploy and maintain. One possible cost-reducing measure follows from the hybrid-fiber coax (HFC) model used for cable television. That is, the bulk of costly and management intensive equipment is centrally located at a hub or head-end. Modulated signals are then distributed between the hub (head-end) and the basestations via optical fiber. The basestations simply contain the electronics (photodiode, amplifiers, antennas) required to translate between the optical and wireless domains.

Various methods of carrying the signal on an optical carrier have been proposed [1]-[7], but few have been tested in a full system. Often, performance has been evaluated with BPSK modulation, a format that has fallen out of use for wireless applications in favor of more complex formats such as QPSK, QAM, and MSK. In this paper, we present a performance limit evaluation of our hybrid fiber/wireless link [8] for a typical deployment. QPSK modulation is considered along with the microwave link budget. For the sake of brevity, only the downlink (basestation to subscriber) is analyzed.

This work was support by the Office of Naval Research (ONR). Eric E. Funk is with SFA, Inc., Largo, MD. P. R. Herczfeld and Maja Bystrom are with Drexel University. Philadelphia, PA, and William Jemison is with Lafayette College, Easton, PA.

II. Downlink Description

A block-diagram view of the downlink being analyzed is shown in Fig. 1. The laser transmitter is located at the LMDS hub. Here, an interface to the network backbone is provided via a broadband modem. The modem generates a QPSK modulated signal that is upconverted to an 8 GHz IF frequency. The IF signal is then sent to a Mach-Zhender modulator (MZM) where it modulates the output of a mode-locked Nd: LiNbO3 microchip laser [9],[10] actively mode-locked with an external reference.

The output from the microchip laser comprises approximately ten mode-locked optical frequencies at an axial mode spacing of f_L= 20 GHz. Modulation of this optical signal via an external modulator at a frequency of f_{IF} = 8 GHz then adds upper and lower modulation sidebands to each of the optical frequencies. At the photodiode the optical frequencies mix with each other to generate a number of electrical beat signals. This self-heterodyne technique yields microwave signals of interest at, $f_{RF} = f_L \pm f_{IF}$ and f_L. The sum frequency (at f_{RF} = 28 GHz) is retained for transmission, while the other frequencies are filtered out.

The modulated signal is distributed over single mode fiber to the remote basestation. At the basestation, a photodiode and requisite filters and amplifiers deliver the signal to a patch antenna. A high gain antenna at the subscriber receiver delivers the signal to a MMIC based down-converter, converting the signal to an IF frequency for delivery to the modem.

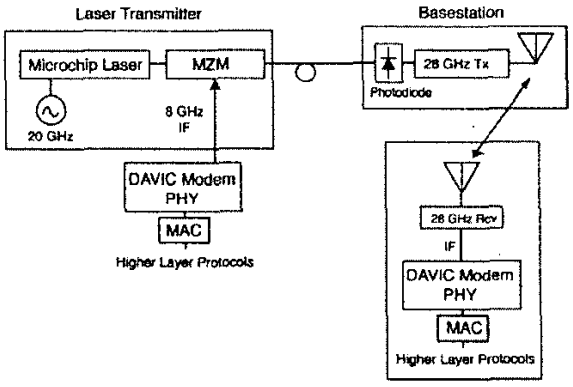

Fig. 1. Downlink Layout

This particular analysis considers only the stationary system. The link budget, modulation, and coding requirements would be entirely different if a multi-path mobile environment were considered.

III. Modem Description

The reference modem for this system analysis is based on the DVB/DAVIC [11] physical layer for LMDS, with the exception that a smaller 6 MHz channel bandwidth has been chosen. The reduced bandwidth conforms to readily available cable-modem equipment.

The functionality of the downstream modem is as follows. The transmitting modem packages incoming data into 188 byte MPEG2-Transport Stream (MPEG2-TS) Packets. The data is randomized for the purpose of spectral shaping, followed by Reed-Solomon (RS) Forward Error Correction (FEC) coding, and interleaving. Finally, the data is mapped to a conventional Grey coded QPSK constellation. Filtering with a raised root cosine (RRC) filter is applied in order to minimize inter-symbol interference [13]. The IF signal is then sent on to be multiplexed with other channels and modulated onto the optical carrier as shown in Fig. 1.

Table I contains a tabulation of the channel throughput based on our chosen parameters.

TABLE I
CHANNEL THROUGHPUT CALCULATION

Parameter	Value
Channel Bandwidth	6 MHz
Raised Root Cosine Filter (α)	0.2
Symbol Rate	5.0 MBaud
Channel Bit Rate	10 Mb/s
Coding Efficiency RS(204,188)	0.92
Channel Throughput	9.2 Mb/s

In our analysis, we assume that the modem provides optimal coherent detection (hard decision) with a matched filter. Since the system is fixed wireless, the channel impulse response is taken to be time-invariant. With these assumptions, the uncorrected symbol-error-rate, P_e, of the AWGN channel for a QPSK signal is bounded as follows [12]-[13]:

$$P_e < erfc\left(\sqrt{\frac{C}{2N}}\right), \qquad (1)$$

where (C/N) is the carrier to noise ratio (CNR). Significant improvement in the RF channel error rate is provided by FEC. The RS(204,188) code, shortened from an RS(255,239) code, was selected to be compatible with ITU/ETSI wireless standards. It is implemented byte-wise, and provides up to eight error corrections within a 204-byte block. With FEC applied, we calculate that a CNR of 11 dB bounds the corrected bit error rate at $<10^{-10}$, an acceptable fiber-quality rate.

IV. Optical Link Analysis

Our optical link contains the following possible sources of impairment to our wireless signal: laser phase noise, laser amplitude noise, photoreceiver thermal noise, and fiber dispersion. In this case, we will assume that the link is short-haul such that fiber dispersion is negligible.

The effect of these other noise sources can be quantified via some straightforward measurements. The measured single sideband (SSB) residual and absolute phase noise of our laser is shown in Fig. 2. Note that the absolute phase noise essentially tracks the phase noise of the 20 GHz source to which the laser is locked.

A similar measurement of laser amplitude noise is shown in Fig. 3. Note that discrete spurious signals are displayed seperately. The spectrum is dominated by a discrete spurious signal of —35 dBc at 460 kHz offset. This is likely due to the laser s relaxation oscillation. The amplitude noise power spectral density is also enhanced near this peak.

The level of impairment caused by each of these noise sources can be estimated by integrating the amplitude and phase noise plots over the bandwidth of interest. In choosing the region of integration, we note that the automatic gain control in the modem will act as a high pass filter to amplitude noise while the phase locked loop carrier recovery will act as a high pass filter to phase noise. We assume a typical high-pass cutoff for both of these effects of 10 kHz. In addition, we assume that the receiver matched filter will act as a low-pass filter with 6 MHz cutoff. Hence, we integrate the noise power spectral densities from 10 kHz to 6 MHz, carefully accounting for the single-sideband nature of the phase noise measurement. The resulting noise levels are tabulated in Table II together with the measured photoreceiver thermal noise level. This yields a total optical link noise level of —23 dBc.

From Table II, it is clear that thermal and amplitude noise will be a greater source of impairment than phase noise. We also note that the photoreceiver relative thermal noise level could be reduced below the amplitude noise level with improved fiber coupling and/or additional laser power.

These noise sources can be included in the microwave link budget through a calculation of implementation loss. The implementation loss represents the excess transmitter power required to maintain a fixed error-rate when compared to an ideal noise-free transmitter. Based on our measured noise levels, and a post-FEC bit error rate of 10^{-10}, an implementation loss of 0.5 dB is calcuated for the optical link as shown in Table II.

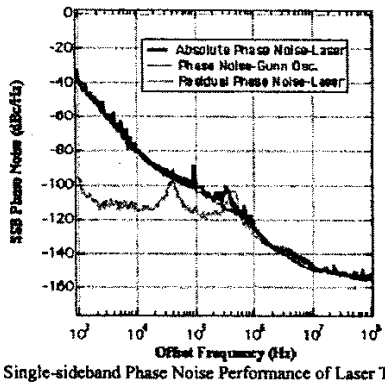

Fig. 2. Single-sideband Phase Noise Performance of Laser Transmitter

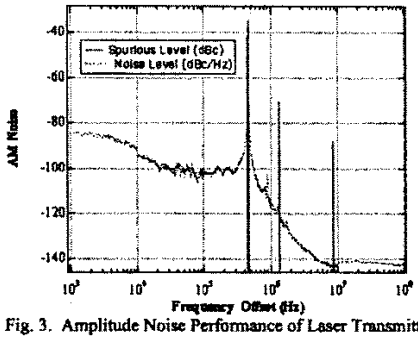

Fig. 3. Amplitude Noise Performance of Laser Transmitter

TABLE II
OPTICAL LINK IMPLEMENTATION LOSS

Noise Source	Level
Integrated Amplitude Noise (laser)	-27 dBc
Laser Relaxation Oscillation (tone)	-35 dBc
Integrated Absolute Phase Noise (laser)	-38 dBc
Integrated Thermal Noise (photoreceiver)	-26 dBc
SUM OPTICAL LINK NOISE	-23 dBc
Microwave Link Noise (budgeted)	-11.5 dBc
TOTAL NOISE LEVEL ($<10^{-10}$ BER)	-11 dBc
Optical Implementation Loss (Microwave Link Noise less Total Noise)	0.5 dB

Next, measurements of error-vector magnitude (EVM) [14] were used to further quantify the performance of the optical link. Unlike the more typical bit-error-rate measurement, an EVM measurement can easily distinguish between amplitude and phase impairments, allowing us to correlate the EVM measurement with the noises tabulated in Table II.

The vector analysis test setup is shown in Fig. 4. The external MZM following the mode-locked microchip laser is driven by an amplified test modulation signal generated by an Agilent 4431B vector signal source. The signal-to-noise ratio (SNR) of the modulated signal feeding the MZM was 48 dB. The vector-modulated signal was delivered across the optical link and received by the photo-receiver. The microwave signal was then down-converted to a 344 MHz intermediate frequency via an HP7004 low-noise microwave down-converter. The down-converted signal was then sent to an Agilent vector signal analyzer (VSA), which demodulates the signal and provides plots of the signal constellation as well as a quantitative measurement of EVM.

Note that the RF carrier frequency used in the EVM measurements was 22 GHz; however similar performance would be expected at the 28 GHz LMDS frequency.

The first vector analysis was performed by sending a North American Digital Cellular (NADC) standard $\pi/4$ DQPSK modulation across the link at 49 Kb/s. An excellent EVM of 7% was measured as shown in Fig. 5(a), illustrating that the link is almost transparent to this legacy wireless standard.

Since the data rates of many of the legacy wireless standards are quite low, we reserved our detailed vector signal analysis for broadband signals that are more representative of LMDS and millimeter-wave radio. Hence, the signal source was now programmed to reproduce the 6 MHz bandwidth signal as specified in Table I.

The measured constellation for the LMDS QPSK signal of Table I is shown in Fig. 5(b). Note that the intersymbol paths are not shown in order to facilitate a clear display. A total EVM of 7% rms was measured. The measured EVM *magnitude* error for QPSK was 6% rms.

For comparison, we can now convert our measured amplitude and phase noise levels of Table II from dBc to equivalent *rms* levels. Assuming that thermal noise contributes equally to amplitude and phase error, we calculate a total predicted EVM of 7% rms with a 6% rms magnitude component. As expected, this agrees exactly with the measured EVM of Fig. 5, implying that there are no other significant sources of impairment.

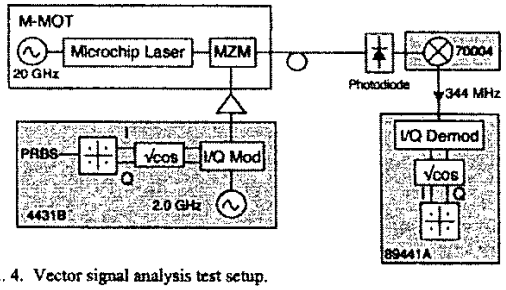

Fig.. 4. Vector signal analysis test setup.

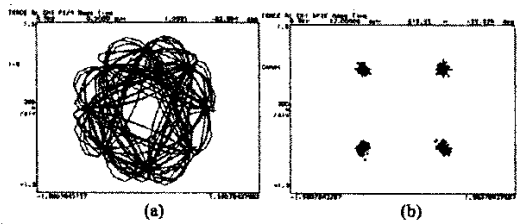

Fig. 5. Measured Constellations: (a) $\pi/4$ DQPSK (NADC) EVM= 7% rms, (b) QPSK (LMDS), EVM= 7% rms, 6% rms magnitude

V. Microwave Link Analysis

Our link budget is based upon a target 11 dB CNR as required for a less than 10^{-10} post-FEC error rate. Currently, cost effective transmitters using off-the-shelf MMIC devices yield transmitters with a 1-dB output compression point between 20 and 30 dBm. In order to control inter-modulation distortion impairments in a multi channel system, we require a significant power back-off for optimal performance. Hence, we will limit our transmitter microwave power to 10 dBm.

The antenna gain is our next consideration. Typically an LMDS basestation will serve a sectored cell with 90 degree sectors and a corresponding 14 dBi of antenna gain [15]. On the subscriber side, the antenna is pointed directly at the base-station via line-of-sight, and a much higher gain is used. 36 dB of gain is typical for the subscriber antenna.

Thanks to the high directivity of the receiver antenna, there is significant rejection of multi-path signal components [16]. However, fading caused by intermittent rainfall must be considered. A rain-fade margin must be set in order to guarantee link availability during heavy rainfall. The required rain-fade margin is based upon system availability requirements and local rainfall statistics. For high quality service, a link that is available 99.99% of the time is specified. In the Washington, DC area, rainfall statistics require an excess link margin of 15.7 dB/km [15] for 99.99% availability.

Computing path loss [17] and adding in rainfall attenuation, the power at the receiving antenna is calculated as shown in Table III. Similarly, the effective noise power (referenced to the receiving antenna terminals) is also tabulated. Allowance is given for an effective microwave noise figure of 4 dB. An additional 0.5 dB of optical implementation loss (as discussed in Section IV) is added along with a 2 dB margin for modem implementation loss and other losses. The CNR is then calculated to verify that our required 11 dB CNR is met. We note that a line-of sight path length of <1.51 km will allow us to meet or exceed our target bit-error-rate of 10^{-10} with an effective CNR of 11 dB.

VI. Conclusion

We have presented a physical layer analysis of an LMDS system employing optical generation and fiber-optic delivery of the millimeter wave carrier. We have found that optical layer impairments due to phase noise and amplitude noise result in less than 1 dB of implementation loss. The optical link performance was further verified by vector signal measurements that agree with the measured amplitude and phase noise levels. Furthermore we have developed a link budget for a typical deployment scenario including the effects of rainfall attenuation.

This analysis is designed to serve as a baseline in the continuing development of hybrid/fiber wireless system previously demonstrated [8]. Enhancements to the current system being considered include development of an Erbium doped Lithium Niobate laser, moving the optical link to the more common 1.55 μm wavelength and integration of the MZM modulator with the laser.

TABLE III
Microwave Link Budget

Carrier	
Transmitter Power	10.0 dBm
Transmitter Antenna Gain	14.0 dB
Path Loss (1.51 km, 28 GHz)	-125.0 dB
Rain Fade (-15.7 dB/km)	-23.7 dB
Receive Antenna Gain	36.0 dBi
SUM CARRIER POWER:	-88.7 dBm
Noise	
kBT (6 MHz Bandwidth, 300 K)	-106.2 dBm
Microwave Noise Figure	4.0 dB
Optical Implementation Loss	0.5 dB
Modem Implementation Loss	2.0 dB
SUM NOISE POWER	-99.7 dBm
Carrier to Noise Ratio (CNR)	11 dB

References

[1] Z. Ahmed, D. Novak, Rod B. Waterhouse, and Hai-Feng Liu, 37 GHz fiber-wireless system for distribution of broad-band signals, *IEEE Trans. Microwave Theory Tech.*, vol. 45, pp.1431-1435, 1997.

[2] G. H. Smith, D. Novak, C. Lim, and K. Wu, Full-duplex broadband millimeter-wave optical transport system for fibre-wireless access, *Electron. Lett.*, vol. 33, pp. 1159-1160, 1999.

[3] D. Wake, C. R. Lima, P. A. Davies, Optical generation of millimeter-wave signals for fiber-radio systems using a dual mode DFB semiconductor laser, *IEEE Trans. Microwave Theory and Tech.* , vol. 43, pp. 2270-2276, 1995.

[4] J. B. Georges, M. H. Kianf, K. Heppel, M. Sayed, and K. Y. Lau, Optical transmission of narrow-band millimeter-wave signals by resonant modulation of monolithic semiconductor lasers, *IEEE Trans. Microwave Theory and Tech.*, vol. 43, pp. 2229-2240, 1995.

[5] H. Ogawa and Y. Kamiya, Fiber-optic microwave transmission using harmonic laser mixing, and optically pumped mixing, *IEEE Trans. Microwave Theory Tech.*, vol. 39, pp. 2045-2051, 1991.

[6] J. O Reilly and P. Lane, Remote delivery of video services using mm-waves and optics, *J. Lightwave Technol.*, vol. 12, pp. 369-375, 1994.

[7] J. Park, and K. Y. Lau, Millimeter—wave (39 GHz) fiber-wireless transmission of broadband multi-channel compressed digital video, *Electron. Lett.*, vol. 32, pp. 474-476, 1996.

[8]W. D. Jemison, P. R. Herczfeld, W. Rosen, A. Vieira, A. Rosen, A. Paolella, and A. Joshi, Hybrid Fiberoptic-Millimeter-Wave Links, *IEEE Microwave Magazine*, vol. 1, pp. 44-51, 2000.

[9] A. Viera, and P. R. Herczfeld, 20 GHz mode-locked Nd:LiNbO3 microchip Laser, in *Proc. Conference on Laser and Electro-Optics/Quantum electronics and Laser Science*, pp.141-142, May 1997.

[10] A. Viera, and P. R. Herczfeld, Microchip laser for microwave and millimeter wave generation, in *Proc. 1997 SBMDO/IEEE MTT-S International Microwave and Optoelectronics Conference*, pp. 333-337, August 1997.

[11] Digital Audio Visual Council, DAVIC 1.4.1 Part 8 (Lower Layer Protocols and Physical Interfaces), 1999.

[12] Mohsen Kavehrad, and Emil Savov, Fiber-Optic Transmission of Microwave 64-QAM Signals, *IEEE Journal on Selected Areas in Communications*, vol. 8, pp.1320-1326, 1990.

[13] John G. Proakis, *Digital Communications*, New York: McGraw Hill, 1995, Ch. 5.

[14] Using vector modulation analysis in the integration, troubleshooting, and design of digital RF communications systems, HP Product Note HP89400-8.

[15] LMDS-The Wireless Interactive Broadband Service, HP Application Note 1296.

[16] Harry R. Anderson, Estimating 28 GHz LMDS Channel Dispersion in Urban Areas Using a Ray-Tracing Propagation Model, *1999 IEEE MTT-S Symposium on Technologies for Wireless Applications*, pp. 111 —116, 1999.

[17] H. T. Friis, A Note on a Simple Transmission Formula, *Proc. IRE* , vol. 34, pp. 254-256, 1946.